TRANSITIONAL FREE CONVECTION FLOW AND HEAT TRANSFER WITHIN ATTICS IN COLD CLIMATE

Huimin CUI[1-3,*], Wenyue WANG[1], Feng XU[4], Suvash C. SAHA[5], and Qingkuan LIU[2,3,6]

[*1]Department of Mathematics and Physics, Shijiazhuang Tiedao University, Shijiazhuang 050043, China

[2]State Key Laboratory of Mechanical Behavior and System Safety of Traffic Engineering Structures, Shijiazhuang Tiedao University, Shijiazhuang 050043, China

[3]Innovation Center for Wind Engineering and Wind Energy Technology of Hebei Province, Shijiazhuang 050043, China

[4]School of Civil Engineering, Beijing Jiaotong University, Beijing 100044, China

[5]School of Mechanical and Mechatronic Engineering, Faculty of Engineering and Information Technology, University of Technology Sydney, Ultimo NSW 2007, Australia

[6]School of Civil Engineering, Shijiazhuang Tiedao University, Shijiazhuang 050043, China

[*] Corresponding author; E-mail: huimincui@stdu.edu.cn

The transitional free convection flow and heat transfer within attics in cold climate are investigated using three-dimensional numerical simulations for a range of Rayleigh numbers from 10^3 to 10^6 and height-length ratios from 0.1 to 1.5. The development process of free convection in the attic could be classified into three stages: an initial stage, a transitional stage and a fully developed stage. Flow structures in different stages including transverse and longitudinal rolls are critically analyzed in terms of the location and strength of convection rolls and their impacts on the heat transfer. The transition to unsteady flow and asymmetry flow in the fully developed stage is discussed for the fixed height-length ratio 0.5. Various flow regimes are given in a bifurcation diagram in the parameter space of Rayleigh numbers ($10^2<Ra<10^7$) for height-length ratios ($0.1<A<1.5$). The time series of heat transfer rate through the bottom wall is quantified for different height-length ratios. The overall heat transfer rate for the low Prandtl fluid ($Pr=0.7$) could be enhanced based on three-dimensional flow structure.

Key words*: Transitional flow; Rayleigh number; Convection roll; Height-length ratio; attic space*

1. Introduction

Thermal convection is an important mechanism of flow and heat transfer in nature and technology [1-7]. The work about thermal flows in attics is of basic meaning for the realizing of thermal convection system, and also of actual significance for the architecture of thermal comfort in

buildings. A number of research works have been devoted to free convection and heat transfer in attics[8-11].

The flow in attics is potentially unstable for the cold climate. The experiment showed that transitional convection flows may proceed at a high Rayleigh number(Ra) under the cold climate [12,13]. Additionally, the relation between the Nusselt number and the height-length ratio at various Rayleigh numbers was quantified [14-16]. Poulikakos and Bejan [17] did experiments on the cold climate problem for high Rayleigh numbers. They also obtained some elementary scales of transient free convection[18]. As the Rayleigh number increases, the free convection flow in the attic space experiences a transitional process from symmetry to asymmetry phenomenon in the cold climate [20,21].

Multiple states occurred in attics for the cold climate involving two different fluids (Pr = 0.7 and Pr = 7). Lei et al. conducted the schlieren experiment with the water fluid medium [23,24]. Cui et.al [25] simulated the development process of free convection flows with Pr = 7 in the section-attic cavity in the cold climate in a wide range of Rayleigh numbers [26,27]. These three-dimensional studies above mentioned are focused on the water medium. How does Prandtl number (Pr) affect the appearance of multiple flow states? Do numerous steady states exist for the air medium (Pr = 0.7)? What is the role of Ra and height-length ratio on the symmetry spoiling phenomenon leading to asymmetric flow for the air medium? However, the research on the above questions is not very clear.

Our work attempt to clarify the problems for free convection within the attic space for the cold climate. In this numerical research, the transient development of free convection in attic space is observed for Ra = 10^6. The infulence of Ra on three-dimensional flow, asymmetry and unsteady flow is researched. We also considered the effect of height-length ratio. The research is expected to provide ideas for building thermal design and achieve the purpose of energy saving.

2. Computational model and procedure

The physical system consisted of an attic space of height H, length $2L$, and depth W full of air medium as illustrated in Fig. 1. The inner walls of the attic are set as non-sliding walls. Initially, the temperature of air in the attic was T_0. At an initial time, the bottom wall is heated and keeps it at a higher temperature T_H, while the two top walls are cooled and stay at a lower temperature T_C. The other two vertical walls are insulated. We assumed that the medium behaves as an ideal gas. The thermal conductivity κ, specific heat capacity, and viscosity are set as constants and calculated at the reference temperature $T_0 = (T_h+T_c)/2$. It have been demonstrated that three-dimensional Navier-Stokes equations and energy equation with Boussinesq approximation could describe well free convection in attics. The scales are summarized as follows: $x, y, z \sim H$; $t \sim H^2/(\kappa \mathrm{Ra}^{1/2})$; $(T-T_0) \sim (T_h-T_c)$; $u, v, w \sim \kappa \mathrm{Ra}^{1/2}/H$; and $\rho^{-1}\partial p/\partial x$, $\rho^{-1}\partial p/\partial y$, $\rho^{-1}\partial p/\partial z \sim \kappa^2 \mathrm{Ra}/H^3$. The non-dimensional governing equations are expressed as follows:

$$\frac{\partial u}{\partial x}+\frac{\partial v}{\partial y}+\frac{\partial w}{\partial z}=0 \quad (1)$$

$$\frac{\partial u}{\partial t}+u\frac{\partial u}{\partial x}+v\frac{\partial u}{\partial y}+w\frac{\partial u}{\partial z}=-\frac{\partial p}{\partial x}+\frac{Pr}{Ra^{1/2}}\left(\frac{\partial^2 u}{\partial x^2}+\frac{\partial^2 u}{\partial y^2}+\frac{\partial^2 u}{\partial z^2}\right) \quad (2)$$

$$\frac{\partial v}{\partial t}+u\frac{\partial v}{\partial x}+v\frac{\partial v}{\partial y}+w\frac{\partial v}{\partial z}=-\frac{\partial p}{\partial y}+\frac{Pr}{Ra^{1/2}}\left(\frac{\partial^2 v}{\partial x^2}+\frac{\partial^2 v}{\partial y^2}+\frac{\partial^2 v}{\partial z^2}\right)+PrT \quad (3)$$

$$\frac{\partial w}{\partial t}+u\frac{\partial w}{\partial x}+v\frac{\partial w}{\partial y}+w\frac{\partial w}{\partial z}=-\frac{\partial p}{\partial z}+\frac{Pr}{Ra^{1/2}}(\frac{\partial^2 w}{\partial x^2}+\frac{\partial^2 w}{\partial y^2}+\frac{\partial^2 w}{\partial z^2}) \quad (4)$$

$$\frac{\partial T}{\partial t}+u\frac{\partial T}{\partial x}+v\frac{\partial T}{\partial y}+w\frac{\partial T}{\partial z}=\frac{1}{Ra^{1/2}}(\frac{\partial^2 T}{\partial x^2}+\frac{\partial^2 T}{\partial y^2}+\frac{\partial^2 T}{\partial z^2}) \quad (5)$$

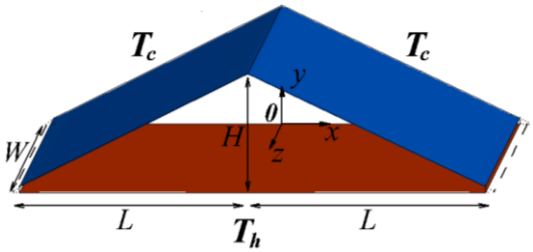

Fig.1. Schematic diagram of computational domain and boundary conditions for A = 0.5[25]

It is expected that free convection flows and heat transfer in attics were controlled by three non-dimensional numbers: the Rayleigh number (Ra), the Prandtl number (Pr) and the height-length ratio (A) [29], which are defined as:

$$\mathrm{Ra}=\frac{g\beta(T_h-T_c)H^3}{\nu\kappa},\quad \mathrm{Pr}=\frac{\nu}{\kappa},\quad A=\frac{H}{L}. \quad (6)$$

Finite volume method was used to solve the governing equations (1) ~ (5), and the pressure-velocity coupling problem was solved by using the SIMPLE scheme. Table 1 showed results of mesh and time step dependence experiments for A = 0.5.We also do similar grid and time step tests for other models with various ratios and Rayleigh numbers. Here, We'll define the mean Nussel number(Nu) in the quasi-steady stage as [17]:

$$\mathrm{Nu}=\frac{1}{S}\iint_S\frac{\partial T}{\partial n}dS \quad (7)$$

Three different non-uniform and symmetric meshes (L×H×W) 110×30×41, 141×41×51 and 171×51×61 and two time steps 0.01 and 0.02 were tested. In order to balance the problem of calculation cost with the accuracy of results of different grids and time steps, the grid of 141×41×51 cells and the time step of 0.02 were adopted in this work.

Table 1. Correlation test results of mesh and time step for A = 0.5

Number	Mesh L×H×W	Time step	Ra = 10^7, Variation of Nu (%)
1	110×30×41	0.02	1.75
2	141×41×51	0.02	—
3	171×51×61	0.02	0.41
4	141×41×51	0.01	0.30

For further verification, the numerical simulation results of the work are compared with the antecedent experiments in Ref. [20], which is shown in Fig. 2. Clearly, the computational result agree well with the experimental result in Fig. 2(b) in Ref. [18]. The quantitative contrast between the numerical test and other published experimental test [13] is also carried out as seen in Fig. 3. At the same position, the temperature difference is less than 10%。

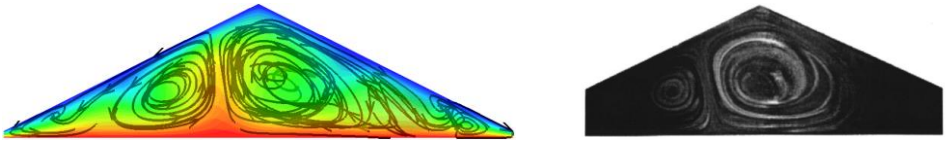

(a) Numerical flow pattern (b) Experimental flow pattern

Fig. 2. The comparsion of numerical and experimental results[14] for Ra = 7×10^4 and A = 0.5

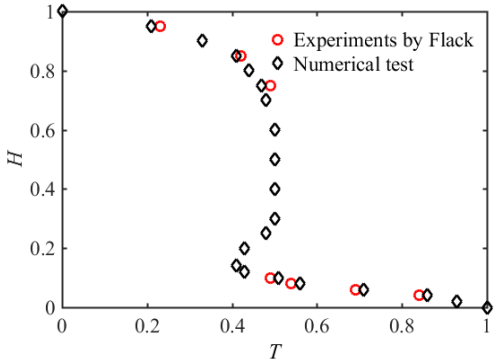

Fig. 3. Contrast between numerical test and the published experimental result [13] for Ra = $2.2x10^5$, A = 1 and Pr = 0.7

3. Transition of Free convection flows

3.1. Transient development of nature convection

The development of transient nature convection for Pr = 0.7 consists of an early, a transitional and a fully development stage, as shown in Fig. 4., which is similar to that for Pr = 7 [25]. The initial stage becomes shorter, and the transitional stage exists earlier and lasts for a long time more than 10s.The Nu for Pr = 0.7 has larger oscillation and approximately twice than that for Pr = 7 in the quasi-steady stage.

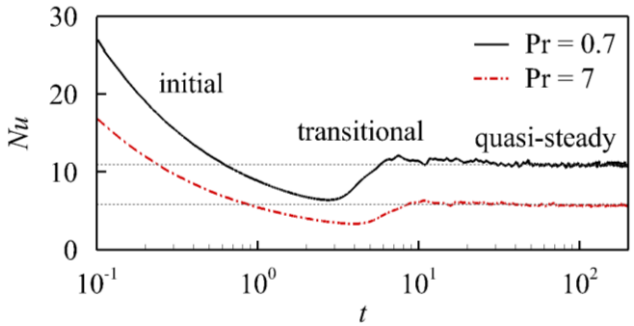

Fig. 4. Time series of Nu for different Prandtl numbers, A = 0.5 and Ra = 10^6(The red dash dot line is for Pr = 7[25]. The black solid line is for Pr = 0.7)

What is the difference of flow structures in different stages for different Prandtl numbers? As shown in Fig. 5 (a), the characteristics of the flow in the early stage is the formation of a thermal boundary layer around the wall surfaces. During transition stage, the intrusion flow near the bottom surface begins to form at t = 8, as shown in Fig. 5(b). Oppositely moving intrusion streams meet to form upward moving thermal plumes.We can find that the heated plumes ascend in the middle of the attic, and cooled plumes descend near the tip region from Fig.5(c). Compared with the large Prandtl number fluid, the small Prandtl number fluid develops slowly [26,27]. In fully developed stage, the flow is unsteady and three-dimensional, which is more complex than that for Pr=7. The flow

characteristics in the quasi-steady stage will be discussed in the following portion on the basis of the observation of numerical simulation results.

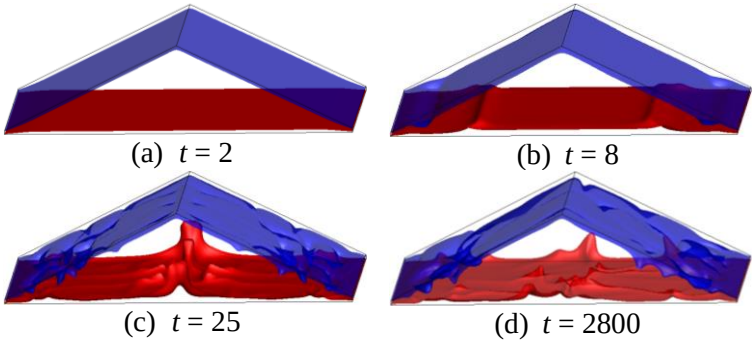

(a) t = 2 (b) t = 8

(c) t = 25 (d) t = 2800

Fig. 5. Temperature iso-surfaces at different times for Ra = 10^6 and A = 0.5 . The bule temperature iso-surface is T = -0.3, the red temperature iso-surface is T = 0.3

3.2. Effect of Rayleigh numbers

For small Rayleigh numbers, the temperature field is stratified, and there are two symmetric transverse rolls in the flow field, as seen in Fig.6. For Ra = 10^4, the isotherms are no longer parallel, and one transverse roll increases and moves toward the center. The short longitudinal rolls form near the tip of the bottom. As Ra goes up, the three-dimensional flow characteristics become more obvious. The longitudinal rolls exist over the entire bottom surface.

The difference of flow configuration in the full development stage shows that the evolution from approximately two-dimensional to three-dimensional and from symmetry to asymmetry. The following paragraphs will describe the convective rolls, asymmetric flows and unsteady flows in the evolutionary stage.

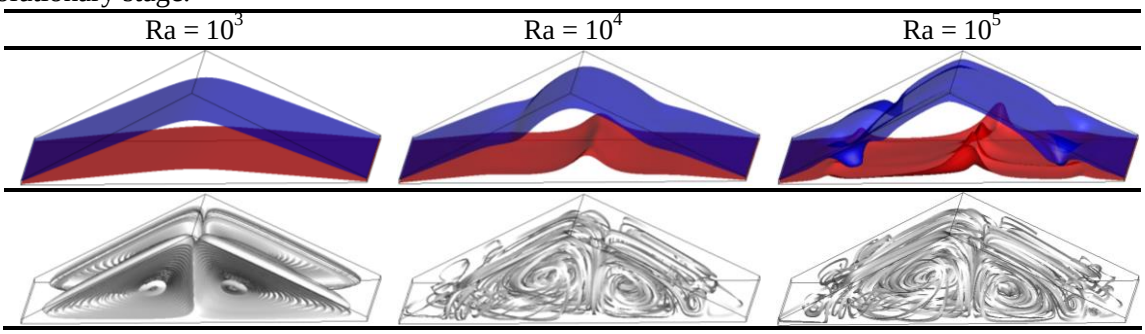

Fig. 6. Temperature iso-surfaces and streamlines in the attic space at t = 2800 in the quasi-steady stage for A = 0.5. The bule surface is the temperature iso-surface of T = -0.3, the red surface is the temperature iso-surface of T = 0.3

3.2.1 Onset of Convection rolls

We will observe the convection rolls from different sections of the attic space. When the Ra is low (Ra = 10^3), the temperature structure of the air in the attic is stratified, and the thermal boundary layer shape (from T = -0.5 to T = -0.4) is very clear in Fig.7. The flow is driven by buoyancy force near the inclined wall, and the flow is in the state of steady laminar and its intensity is weak. The weak basic flow is considered as a two-dimensional flow in the attic space.

As Ra increases (Ra = 10^4) , one of transverse rolls increases in size and move toward the middle of the attic. Another transverse roll remains but diminishes in size. The secondary transverse

roll forms in the corner region near the large convective roll. The apparent asymmetry is clearly different from that of water medium [26]. When Ra further increases above the critical value, the flow patterns become more asymmetric and the number of secondary vortices have a tendency to increase. For Ra = 10^5, the secondary transverse roll breaks up and occupys the entire tip region.

At Ra = 10^6, the asymmetry phenomenon is obvious. The secondary transverse rolls increase in number, appear throughout the attic space and superimpose on two large transverse rolls. These transverse rolls have reduced length and irregular shape. In this case, the boundary layers at the region of inclined surface and bottom surface become thinner.

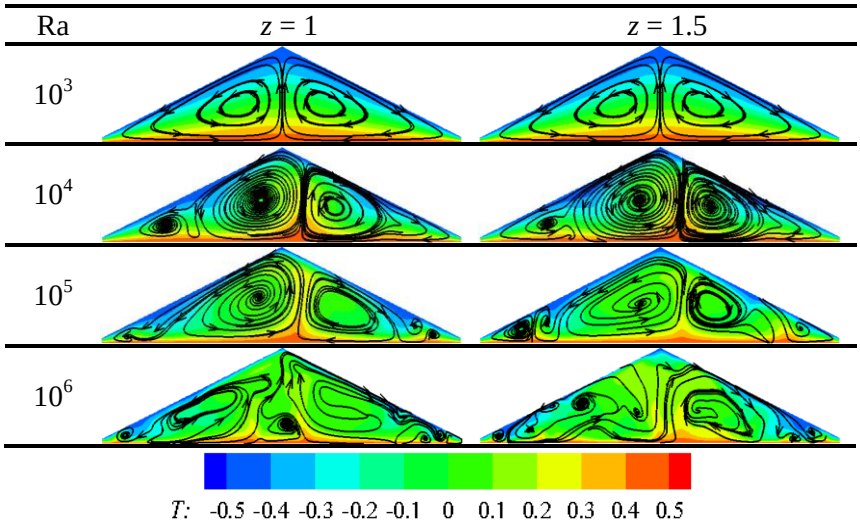

Fig. 7. Isotherms and streamlines in the *xy*-cross section at different locations in the fully developed stage (t = 2800) for A = 0.5

In order to observe longitudinal rolls, Fig. 8 shows isothermals and streamlines in different *yz*-cross sections with Ra from 10^3 to 10^5. For Ra = 10^3, they are similar to those for the water medium (see [32-34] for details). As Rayleigh number increases, weak cells appear nearby two vertical walls in the *yz*-cross section (x = 0.5) when Ra is 10^4. With the Ra further development, longitudinal rolls appear near the vertical sidewalls, as seen in the *yz*-cross section (x = 1) for Ra = 10^5. The length of longitudinal rolls is not large, because the longitudinal rolls don't exist in the plane x = 1. The horizontal flow at the bottom of the region, creating longitudinal convection rolls, like the formation mechanism of Rayleigh-Bénard-Poiseuille flow[23]. However, the longitudinal rolls in attics are more irregular in shape than that for the water medium, especially for higher Rayleigh numbers.

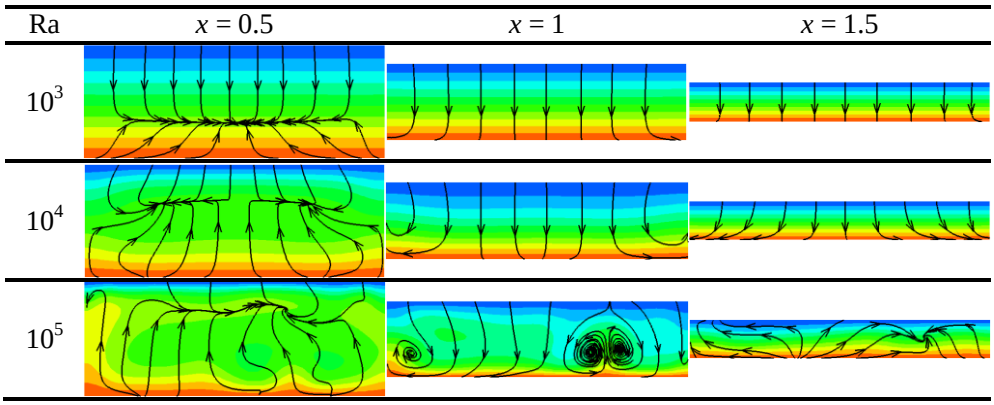

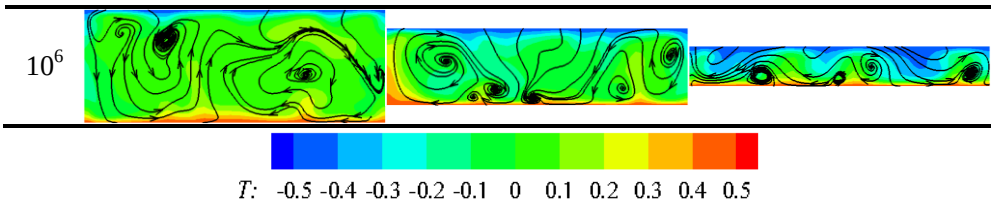

Fig. 8. Isotherms and streamlines in the *yz*-cross section at different locations in the fully developed stage (t = 2800) for A = 0.5

Fig. 9 shows dependence of the averaged vorticity for different Rayleigh numbers.We define the mean vorticities in *x*-, *y*- and *z*-direction in the quasi-steady stage as [24]:

$$\Omega_x = \frac{1}{V}\iiint_V \left|\frac{\partial w}{\partial y} - \frac{\partial v}{\partial z}\right| dV, \quad (8) \qquad \Omega_y = \frac{1}{V}\iiint_V \left|\frac{\partial w}{\partial x} - \frac{\partial u}{\partial z}\right| dV, \quad (9)$$

$$\Omega_z = \frac{1}{V}\iiint_V \left|\frac{\partial v}{\partial x} - \frac{\partial u}{\partial y}\right| dV, \quad (10) \qquad \Omega_t = \Omega_x + \Omega_y + \Omega_z. \quad (11)$$

Here, We can use the vorticity of Ω_x, Ω_t and Ω_z to quantitatively describe longitudinal rolls, transverse rolls and total rolls respectively (also see [24]). When Ra is less than 10^3, the magnitude of vorticity is almost zero. The onset of RB convection rolls lead to an increase in vorticity Ω_z around $Ra_{TR} = 10^3$ for A = 0.5. Moreover, the critical Rayleigh number at the start of longitudinal rolls is about $Ra_{LR} = 1.3\times10^4$, which is smaller than that for the water medium. The strength of the total rolls significantly increase around Ra = 3×10^4, and the value of Ω_z is lower than that for the water medium.

3.2.2 Transition to asymmetry flow

The asymmetry flow in the attic space is obvious in Fig. 7. As a results of pitchfork bifurcation, the transition from symmetry to asymmetry flows around the geometric central plane appears[29,21,24,25]. As defined in the previous study [21], the asymmetry flow in the attic is calculated use the degree I:

$$I = \frac{\iiint_V [T(x,y,z) - T(-x,y,z)]^2 dV}{4\iiint_V [T(x,y,z)]^2 dV}. \quad (12)$$

Fig. 10 shows the values of I with different Rayleigh numbers at range of Ra = 10^2 to 10^7. Clearly, I significantly increases around $Ra_I = 9\times10^3$. This implies that the critical Rayleigh number Ra_I from symmetry to asymmetry flows is smaller than that for the water medium. The value of I quantifying the asymmetry flow is almost 3-orders higher than that of water medium.

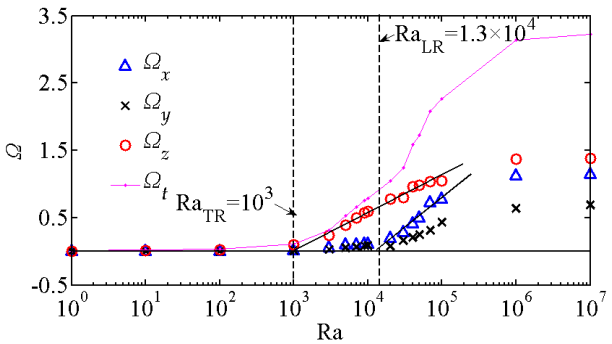

Fig. 9. The dependence between mean vorticity and the Rayleigh number for A = 0.5 and Pr = 0.7

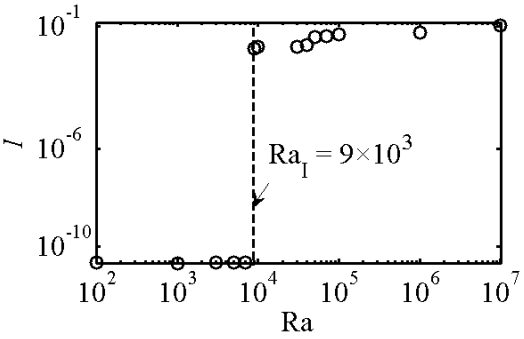

Fig. 10. The dependence between the degree of symmetry I and Rayleigh numbers, A = 0.5

3.2.3 Transition to oscillatory convection

In this section, the height-length ratio of the attic is 0.5. The numerical results show that there is no oscillation in the states of the three transverse rolls at Ra = 3×10^4. The temperature at the monitoring points in Fig.11(a) has not changed over time. Small perturbations appear in the temperature time series at Rayleigh number 3.4×10^4, as illustrated in Fig. 11(b). The meaning is the transition from steady to unsteady flow state occurs around $Ra_{US} = 3.4\times10^4$.

For observing the characteristics of unsteady flow and demonstrate its transition to turbulence, Fig. 11(c) shows the PSD(power spectrum density) of the periodic flow in the full development stage for Ra = 3.4×10^4, and the main frequency (f_p = 0.0004) and harmonic frequencies are clear. The peak frequency on the spectrum is consistent. As the Rayleigh number increases, the flow is still periodic, but the peak frequency changes with f_p = 0.0011 at P1 and f_p = 0.0005 at P3(P3′) for Ra =4×10^4(see Figs. 11 (d,e)). In addition, subharmonic frequencies appear in the spectrum diagram.

The chaotic flow appears near Ra = 5×10^4. The temperature time series and the corresponding PSD are plotted in Figs. 11(f,g). There is no clear dominant peak frequency and harmonic frequency in this mode. This indicates that the flow occurs chaotic. The Rayleigh number of flow transition to chaos in the attic with water medium is one order of magnitude higher than that of air medium. Current studies show that the change of Prandtl number has a significant effect on the critical Rayleigh number of flow evolution, its construction,frequency time evolution and space evolution.

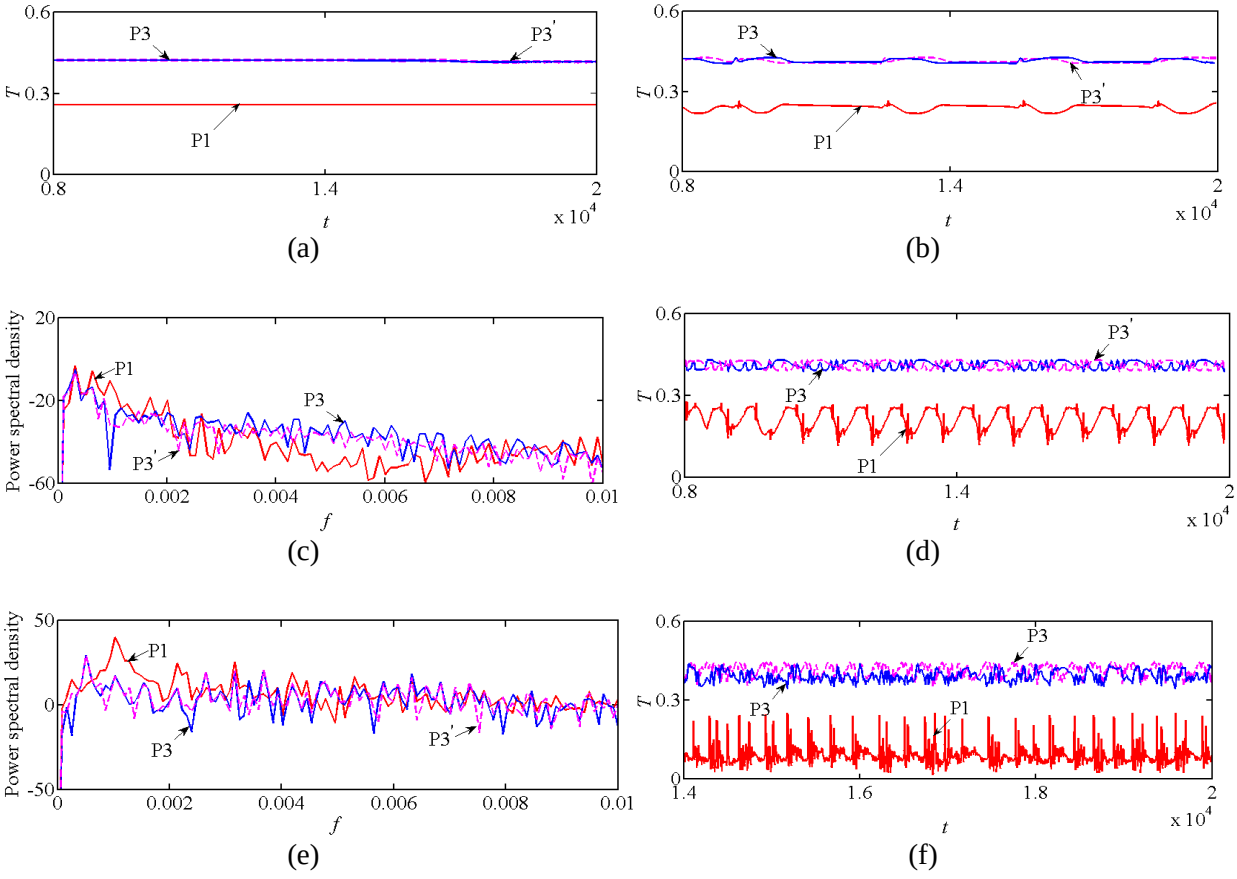

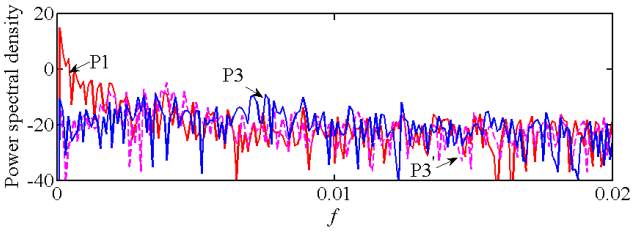

(g)

Fig. 11. Temperature time series and PSD of the convection at P1 (0, 0.5, 1), P3 (-0.54, 0.11, 1), P3' (0.54, 0.11, 1) with different Rayleigh numbers. (a) Ra = 3×10^4, (b) and (c) Ra = 3.4×10^4, (d) and (e) Ra = 4×10^4, (f)and(g) Ra = 5×10^4.

3.3. Flow regime

According to the above analysis, it can be obtained that the two-dimensional symmetric steady-state firstly appears in the triangular attic under low Rayleigh numbers, as shown in Region I in Fig. 12. Region I can be divided into a Basic flow region. The flow in this region is driven by the fluid near the cooling inclined walls and forms two symmetrical transverse convective rolls with opposite rotational directions. As Rayleigh number increases, the Rayleigh-Bénard(RB) instability strengthens the intensity of the transverse convective rolls, and the instability in the triangular attic with the lower height-length ratio makes the convective rolls bifurcating into many pairs.

For small height-length ratio (A < 0.5) and large height-length ratio (A > 1.1) of the attic space, as the Rayleigh number gets bigger, the flow presents a three-dimensional symmetric steady state(Region II), followed by the three-dimensional asymmetric steady state(Region III). The three-dimensional flow in the attic with small height-length ratio is mainly the longitudinal convective rolls, while the three-dimensional flow in the attic with large height-length ratio is mainly the RB convective cell. With the increases of Rayleigh number in the attic that the height-length ratio between 0.5 and 1.1, the flow firstly presents a two-dimensional asymmetrical steady state(Region IV), and then a three-dimensional asymmetrical steady state(Region III).

For all height-length ratios, as the Rayleigh number continues to grow, the flow in attics presents a turbulent state, as shown in Region V. The critical Rayleigh number of this state is positively correlated with the height-length ratio.

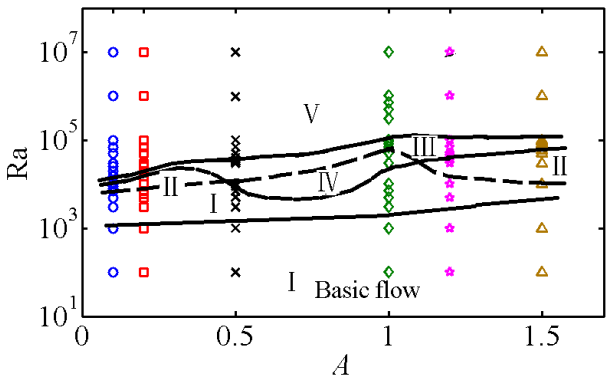

Fig. 12. A state diagram of the observed patterns in triangular cavities with different Rayleigh numbers and height-length ratios and Pr = 0.7. Region I is the two-dimensional symmetrical steady flow, Region II is the three-dimensional symmetrical steady flow, Region III is the three-dimensional

asymmetrical steady flow, Region IV is the two-dimensional asymmetrical steady flow and Region V is the three-dimensional asymmetrical unsteady flow

4. Heat transfer

As the height-length ratio increase, the evolution tendency of Nusselt number over time is similar, seen in Fig.13. However, the time reaching the quasi-steady state is gradually delayed, and the value of Nusselt number gradually is increased. In the fully developed stage, the fluid flow is unsteady for A = 0.1 and 0.2. For the attic with smaller height-length ratio, the flow reaches an unsteady state at lower Ra number.

As shown in Fig.14, the Nusselt number of the bottom surface is slightly larger than that of the top surface, which is analogous to the two-dimensional simulation result [24]. The Nusselt number increases as the Rayleigh number increases. How does the Nusselt number change with Rayleigh number? The fitting results of three-dimensional numerical simulations are higher than $Nu \sim Ra^{1/3}$, which is accordance with the heat transfer law in RB convection [35,36]. This maybe caused by the existence of longitudinal convection rolls in the attics.

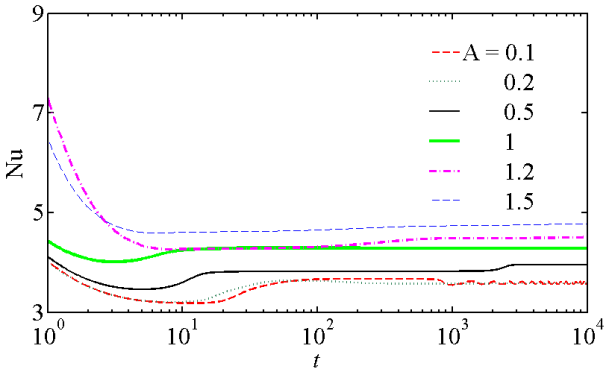

Fig. 13. The Nusselt number of the bottom wall changes over time for different height-length ratios at Ra = 10^4

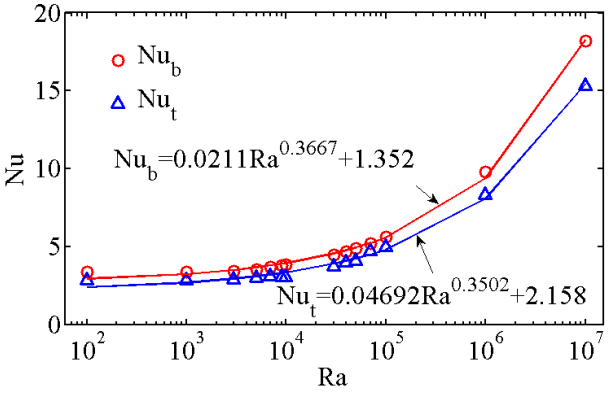

Fig. 14. Graph of the Nusselt number as a function of the Rayleigh number at the bottom wall and the top wall for A = 0.5 and Pr = 0.7

5. Conclusions

This paper focuses on the evolution of different flow states and their impact on the physics of heat transfer in attics. The transient stages are relatively earlier than those for the water medium. In the quasi-steady stage, the three-dimensional flow structures in the quasi-steady stage depend on what the Rayleigh number is. These Rayleigh numbers including Ra_{TR}, Ra_{LR} and Ra_I are lower than those for the water medium. Nevertheless, the asymmetry phenomenon is more obvious due to the large scale movement of the transverse rolls. The transition to an unsteady flow state largely depends on the appearance of three-dimensional flow. The critical Rayleigh number of the unsteady phenomenon in the attic space is significantly lower than that for larger Prandtl number. In the Ra-A regime diagram, the two-dimensional asymmetrical steady flow state exists, which is not observed in other studies. Heat transfer rate in attic space increase as the height-length ratio and Rayleigh number increase. The relation between Nu and Ra is higher than $Nu \sim Ra^{1/3}$. It demonstrates that the flow structure in three dimensions is helpful in heat transfer.

For the first time, the distribution of flow patterns in the attic space has been shown in the control parameter space based on numerical simulation, which has guiding significance for understanding the flow mechanism in the cavity. The variation of heat transfer law in the attic with the aspect ratio and Ra number is given, which is instructive to the thermal design of buildings. Further experimental results of three-dimensional flow structure in attics will be given in the future.

Acknowledgements

The study is financially supported by National Natural Science Foundation of China (11802186, 5177838), Natural Science Foundation of Hebei Province (E2018210113, E2018210044) and Department of Education of Hebei Province (BJ2019004).

Nomenclature

A	height-length ratio
g	gravitational acceleration [ms–2]
H, L, W	height, half length and width of the attic(m)
k	thermal conductivity(Wm-1K-1)
n	coordinate normal to the wall
Nu	Nusselt number
Nu_b	Nusselt number of the bottom
Nu_t	Nusselt number of the top
p	nondimensional pressure
Pr	Prandtl number
Ra	Rayleigh number
Ra_I	critical Rayleigh number for appearance of the asymmetry flow
Ra_{LR}	critical Rayleigh number for appearance of longitudinal rolls
Ra_{TR}	critical Rayleigh number for transverse rolls dominated by RB convection
Ra_{US}	critical Rayleigh number for appearance of the unsteady flow
s	coordinate along the wall
S	area of the wall(m2)
t	nondimensional time scale
T	nondimensional temperature
T_0	initial temperature(K)
T_c, T_h	temperatures of the cold inclined top and the hot bottom(K)
u, v, w	nondimensional x-, y- and z-velocity
V	volume of the attic(m3)
Ω_t	the total averaged magnitude of vorticity(s-1)
Ω_x, Ω_y,Ω_z	the averaged magnitude of vorticity in the x- , y-and z-direction(s-1)
x, y, z	nondimensional coordinate
Greek symbols	
β	coefficient of thermal expansion(mK-1)
ΔT	temperature difference between the bottom and the top wall(K)
κ	thermal diffusivity(m2s-1)
ν	kinematic viscosity(Nsm-2)

ρ medium density(kgm-3)

References

[1] R. Kessler, Nolinear transition in three-dimensional convection, *J. Fluid Mech*. 174 (1987) 357-379.

[2] J. Ma, B.C. Nie, F. Xu, Pr > 1 unsteady thermal flows and heat transfer in a finned cavity with a uniform heat flux, *Int. J. Therm. Sci*. 129 (2018) 83-93.

[3] H.Y. Zhai, B.C. Nie, B. Chen, F. Xu, Unsteady flows on a roof imposed by a periodic heat flux: 2D simulation and scaling analysis, *Int. J. Therm. Sci*. 145 (2019) 106002.

[4] E. F. Kent. Numerical computation of laminar natural convection in triangular shaped cavities, *Adv. Appl. Mech. XIII* 128 (2020) 27-38.

[5] E. F. Kent.Numerical analysis of laminar natural convection in isosceles triangular enclosures for cold base and hot inclined walls, *Mech. Res. Commun.* 36 (2009) 497-508.

[6] D. Das, M. Roy, T. Basak. Studies on natural convection within enclosures of various (non-square) shapes-A review, *Int. J. Heat Mass Transfer* 106 (2017) 356-406.

[7] A. Rahimi, A. D. Saee, A. Kasaeipoor, E. H. Malekshah. A comprehensive review on natural convection flow and heat transfer: The most practical geometries for engineering applications, *Int. J. Numer. Method. H.* 29 (2019) 834-877.

[8] R.D. Flack, Velocity measurements in two free convection air flows using a laser velocimeter, *J. Heat Transfer* 101 (1979) 256-260.

[9] S.C. Saha, J.C. Patterson, C. Lei, Free convection in attic-shaped spaces subject to sudden and ramp heating boundary conditions, *Int. J. Heat Mass Transfer* 46 (2010) 621-638.

[10] S.C. Saha, Unsteady free convection in a triangular enclosure under isothermal heating, *Energy Build*. 43 (2011) 701–709.

[11] S.C. Saha, Scaling of free convection heat transfer in a triangular cavity for Pr > 1, *Energy Build.* 43 (2011) 2908-2917.

[12] R.D. Flack, T.T. Konopnicki, J.H. Rooke, The measurement of natural convective heat transfer in triangular enclosures, *J. Heat Transfer* 101 (1979) 648-654.

[13] R.D. Flack, The experimental measurement of free convection heat transfer in triangular enclosures heated or cooled from below, *J. Heat Transfer* 102 (1980) 770-772.

[14] H. Asan, L. Namli, Laminar free convection in a pitched roof of triangular cross-section: summer day boundary conditions, *Energy Build.* 33 (2000) 69-73.

[15] T.N. Anderson, M. Duke, J.K. Carson, Experimental determination of free convection heat transfer coefficients in an attic shaped enclosure, *Int. Commu. Heat Mass Transfer* 37 (2010) 360-363.

[16] E.H. Ridouane, A. Campo, Experimental-based correlations for the characterization of free convection of air inside isosceles triangular cavities with variable apex angles, *Exp. Heat Transfer* 18 (2005) 81-86.

[17] D. Poulikakos, A. Bejan, Free convection experiments in a triangular enclosure, *J. Heat Transfer* 105 (1983) 652-655.

[18] D. Poulikakos, A. Bejan, The fluid dynamics of an attic space, *J. Fluid Mech.* 131 (1983) 251-269.

[19] P.M. Haese, M.D. Teubner, Heat exchange in an attic space, *Int. J. Heat Mass Transfer* 45 (2002) 4925-4936.

[20] G.A. Holtzman, R.W. Hill, K.S. Ball, Laminar free convection in isosceles triangular enclosures heated from below and symmetrically cooled from above, *J. Heat Transfer* 122 (2000) 485-491.

[21] E.H. Ridouane, A. Campo, Formation of a pitchfork bifurcation in thermal convection flow inside an isosceles triangular cavity, *Phys. Fluids* 18 (2006) 074102.

[22] E.H. Ridouane, A. Campo, Numerical simulation of the 3D behaviour of thermal buoyant airflows in pentahedral spaces, *Int. J. Heat Fluid Flow* 29 (2008) 1360-1368.

[23] C. Lei, F. Xu, J.C. Patterson, Visualisation of free convection in an isosceles triangular enclosure heated from below, *Proceedings of 55th Pacific Symposium on Flow Visualisation and Image Processing*, Australia (2005).

[24] C. Lei, S.W. Armfield, J.C. Patterson, Unsteady free convection in a water-filled isosceles triangular enclosure heated from below, *Int. J. Heat Mass Transfer* 51 (2008) 2637-2650.

[25] H. Cui, F. Xu, S.C. Saha, A three-dimensional simulation of transient free convection in a triangular cavity, *Int. J. Heat Mass Transfer* 85 (2015) 1012-1022.

[26] H. Cui, F. Xu, S.C. Saha, Transition to unsteady free convection flow in a prismatic enclosure of triangular section, *Int. J. Therm. Sci.* 111 (2017) 330-339.

[27] H. Cui, F. Xu, S.C. Saha, Q. K. Liu, Transient free convection heat transfer in a section-triangular prismatic enclosure with different aspect ratios, *Int. J. Therm. Sci.* 139 (2019) 282-291.

[28] S.C. Saha, M.M.K. Khan, A review of free convection and heat transfer inattic-shaped space, *Energy Build.* 43 (2011) 2564-2571.

[29] C. Lei, J.C. Patterson, A direct three-dimensional simulation of radiation-induced free convection in a shallow wedge, *Int. J. Heat Mass Transfer* 46 (2003) 1183-1197.

[30] S.C. Saha, J.C. Patterson, C. Lei, Free convection in attics subject to instantaneous and ramp cooling boundary conditions, *Energy Build.* 42 (2010) 1192-1204.

[31] S.C. Saha, J.C. Patterson, C. Lei, Free convection and heat transfer in attics subject to periodic thermal forcing, *Int. J. Therm. Sci.* 49 (2010) 1899-1910.

[32] K.R. Kirchartz, H. Oertel JR, Three-dimensional thermal cellular convection in rectangular boxes, *J. Fluid Mech.* 192 (1988) 249-286.

[33] G.M. Horsch, H.G. Stefan, S. Gavali, Numerical simulation of cooling-induced convective currents on a littoral slope, *Int. J. Numer. Meth. Fluids* 19 (1994) 105-134.

[34] C. Lei, J.C. Patterson, A direct three-dimensional simulation of radiation-induced free convection in a shallow wedge, *Int. J. Heat Mass Transfer* 46 (2003) 1183-1197.

[35] W.V.R. Malkus, The heat transport and spectrum of thermal turbulence, *Proc. R. Soc. Lond. A* 225 (1954) 196-212.

[36] S. Grossmann, D. Lohse, Scaling in thermal convection: a unifying theory, *J. Fluid Mech.* 407 (2000) 27-56.

Submitted: 26.08.2021.
Revised: 22.03.2022.
Accepted: 24.03.2022.